

Quintom Wormholes

Peter K. F. Kuhfittig^{*}, Farook Rahaman[†] and Ashis Ghosh[‡]

[†]Department of Mathematics, Milwaukee School of Engineering, Milwaukee, Wisconsin 53202-3109, USA

[‡]Department of Mathematics, Jadavpur University, Kolkata - 700032, India

June 15, 2010

Abstract

The combination of quintessence and phantom energy in a joint model is referred to as quintom dark energy. This paper discusses traversable wormholes supported by such quintom matter. Two particular solutions are explored, a constant redshift function and a specific shape function. Both isotropic and anisotropic pressures are considered.

that much of our Universe is pervaded by a dynamic dark energy that causes the Universe to accelerate [2, 3]: \ddot{a} is positive in the Friedmann equation $\ddot{a}/a = -\frac{4\pi G}{3}(\rho + 3p)$. In the equation of state (EoS) $p = \omega\rho$, a value of $\omega < -1/3$ is required for an accelerated expansion. The range of values $-1 < \omega < -1/3$ is usually referred to as *quintessence* and the range $\omega < -1$ as *phantom energy*. In the latter case we get $\rho + p < 0$, in violation of the weak energy condition, considered to be a primary prerequisite for the existence of wormholes [4, 5, 6]. The special case $\omega = -1$ corresponds to Einstein's cosmological constant. This value is sometimes called the *cosmological constant barrier* or the *phantom divide*.

1 Introduction

A stationary spherically symmetric wormhole may be defined as a handle or tunnel in a multiply-connected spacetime joining widely separated regions of the same spacetime or of different spacetimes [1]. Interest in wormholes was renewed by the realization

The quintessence and phantom energy models taken together as a *joint model* and dubbed *quintom* for short [7] suggests a single EoS, $p = \omega\rho$, to cover all cases. It is shown in Ref. [8], however, that ω cannot cross the phantom divide, that is, in the traditional scalar field model, the EoS cannot cross the cosmological constant barrier. (For further discussion, see Refs. [9, 10, 11, 12, 13].) The simplest quintom model involves two scalar fields, ϕ and ψ , one quintessence-like and one phantom-like

^{*}kuhfitti@msoe.edu

[†]farook_rahman@yahoo.com

[‡]ashis_laru@yahoo.co.in

0

[14, 15]:

$$\mathcal{L} = \frac{1}{2}\partial_\mu\phi\partial^\mu\phi - \frac{1}{2}\partial_\mu\psi\partial^\mu\psi - V(\phi) - W(\psi).$$

So instead of ω in the EoS, we will use ω_q and ω_{ph} , respectively.

One reason for studying quintom dark energy is the bouncing universe [14, 16, 17], which provides a possible solution to the Big-Bang singularity. An extension to the braneworld scenario is discussed in Ref. [18].

The purpose of this paper is to study various wormhole spacetimes that are supported by quintom dark energy. We discuss the structure of such wormholes by means of an embedding diagram, as well as the junction to an external Schwarzschild spacetime. Both isotropic and anisotropic pressures are considered. It is shown that in the isotropic models, the phantom-energy condition $\omega_{ph} < -1$ implies that $\omega_q < -1$, while in the anisotropic case, $\omega_q < -1/3$.

As a final comment, since quintessence satisfies the weak and null energy conditions, it is not feasible to model a wormhole using the quintessence field. So when considered as separate fields, only phantom energy can support a wormhole structure.

2 Construction of quintom wormholes

In the present study the metric for a static spherically symmetric wormhole spacetime is taken as

$$ds^2 = -e^{\nu(r)}dt^2 + e^{\lambda(r)}dr^2 + r^2(d\theta^2 + \sin^2\theta d\phi^2), \quad (1)$$

where $\nu(r)$ and $\lambda(r)$ are functions of the radial coordinate r .

Let us now consider a quintom model, which, as noted earlier, contains a quintessence-like field and a phantom-like field. So we assume that the Einstein field equations can be written as

$$G_{\mu\nu} = 8\pi G(T_{\mu\nu} + \tau_{\mu\nu}), \quad (2)$$

where $\tau_{\mu\nu}$ is the energy-momentum tensor of the quintessence-like field and is characterized by a free parameter ω_q , which is ordinarily restricted by the condition $\omega_q < -\frac{1}{3}$. (Recall that this condition is required for an accelerated expansion.) According to Kiselev [19], the components of this tensor need to satisfy the conditions of additivity and linearity. Taking into account the different signatures used in the line elements, the components can be stated as follows:

$$\tau_t^t = \tau_r^r = -\rho_q, \quad (3)$$

$$\tau_\theta^\theta = \tau_\phi^\phi = \frac{1}{2}(3\omega_q + 1)\rho_q. \quad (4)$$

The energy-momentum tensor compatible with spherical symmetry is

$$T_\nu^\mu = (\rho + p_t)u^\mu u_\nu - p_t g_\nu^\mu + (p_r - p_t)\eta^\mu \eta_\nu. \quad (5)$$

As already noted, a phantom-like field is characterized by the equation of state

$$p_r = \omega_{ph}\rho, \quad (6)$$

where p_r is the radial pressure and $\omega_{ph} < -1$. In the discussion below, p_t is the lateral pressure.

The Einstein field equations in the orthonormal frame are stated next:

$$e^{-\lambda} \left[\frac{\lambda'}{r} - \frac{1}{r^2} \right] + \frac{1}{r^2} = 8\pi G(\rho + \rho_q), \quad (7)$$

$$e^{-\lambda} \left[\frac{1}{r^2} + \frac{\nu'}{r} \right] - \frac{1}{r^2} = 8\pi G(p_r - \rho_q), \quad (8)$$

$$\begin{aligned} \frac{1}{2}e^{-\lambda} \left[\frac{1}{2}(\nu')^2 + \nu'' - \frac{1}{2}\lambda'\nu' + \frac{1}{r}(\nu' - \lambda') \right] \\ = 8\pi G \left(p_t + \frac{(3\omega_q + 1)}{2}\rho_q \right). \end{aligned} \quad (9)$$

3 Model 1: A constant redshift function

For our first model we assume a constant redshift function,

$$\nu(r) \equiv \nu_o = \text{constant}, \quad (10)$$

referred to as the zero-tidal-force solution in Ref. [1]. The absence of tidal forces automatically satisfies a key traversability criterion.

3.1 Isotropic pressure

Our first assumption in the present model is an isotropic pressure:

$$p = p_r = p_t.$$

Adding Eqs. (7) and (8) and using Eqs. (6) and (10), we get

$$e^{-\lambda} \left[\frac{\lambda'}{r} \right] = 8\pi G(\omega_{ph} + 1)\rho. \quad (11)$$

Multiplying Eq. (8) by $(3\omega_q + 1)/2$ and adding to Eq. (9) leads to

$$(e^{-\lambda})' + \frac{A_1 e^{-\lambda}}{r} = \frac{A_1}{r}, \quad (12)$$

where

$$A_1 = \frac{(3\omega_q + 1)(\omega_{ph} + 1)}{(\omega_{ph} + 1) + 3\omega_{ph}(\omega_q + 1)}. \quad (13)$$

The above equation yields

$$e^{-\lambda} = 1 - \frac{D}{r^{A_1}}, \quad (14)$$

where $D > 0$ is an integration constant. We rewrite the metric in the Morris-Thorne canonical form [1], $e^\lambda = 1/[1 - b(r)/r]$, where the shape function is given by

$$b(r) = \frac{D}{r^{A_1-1}}. \quad (15)$$

Using Eqs. (7) and (8), one gets the following forms for ρ and ρ_q :

$$8\pi G\rho = -\frac{DA_1}{(1 + \omega_{ph})r^{A_1+2}} \quad (16)$$

and

$$8\pi G\rho_q = \frac{D(-A_1 + 1 + A_1/(1 + \omega_{ph}))}{r^{A_1+2}}. \quad (17)$$

Observe that $\rho > 0$, since $1 + \omega_{ph} < 0$, while $\rho_q > 0$ implies that $A_1 < (1 + \omega_{ph})/\omega_{ph}$. It follows that $A_1 < 1$.

The assumption $\nu(r) \equiv \nu_o$ implies the absence of a horizon. Also, we would like the wormhole spacetime to be asymptotically flat, that is, $b(r)/r \rightarrow 0$ as $r \rightarrow \infty$. To this end, we require that $A_1 > 0$. From Eq. (13) we deduce that

$$\omega_q < \frac{-4\omega_{ph} - 1}{3\omega_{ph}}.$$

Since $\omega_{ph} < -1$, it now follows that $\omega_q < -1$, thereby having crossed the phantom divide. This result is hardly surprising, given the nature of phantom wormholes. On the other hand, the quintessence condition $\omega_q < -1/3$ is still going to occur, namely in the anisotropic case, discussed next.

3.2 Anisotropic pressure

In the case of an anisotropic pressure, the radial and lateral pressures are no longer equal. In an earlier paper on phantom-energy wormholes, Zaslavskii [4] proposed the form $p_t = \alpha\rho$, $\alpha > 0$, for the lateral pressure. In this manner we obtain simple linear relationships between pressure and energy-density, but with p_r not equal to p_t .

Observe first that Eq. (11) remains the same. After multiplying Eq. (8) by $(3\omega_q + 1)/2$ and adding to Eq. (9), we get, analogously,

$$(e^{-\lambda})' + \frac{A_2 e^{-\lambda}}{r} = \frac{A_2}{r}, \quad (18)$$

where

$$A_2 = \frac{(3\omega_q + 1)(\omega_{ph} + 1)}{(\omega_{ph} + 1) + 2\alpha + \omega_{ph}(3\omega_q + 1)}. \quad (19)$$

Otherwise Eqs. (14)-(17) retain their form.

As before, we want $A_2 > 0$. So from Eq. (19), we have

$$\omega_{ph} + 1 + 2\alpha + \omega_{ph}(3\omega_q + 1) > 0$$

and

$$\omega_q < \frac{-2\omega_{ph} - 1 - 2\alpha}{3\omega_{ph}}. \quad (20)$$

Since $\alpha > 0$ and $\omega_{ph} < -1$, it follows that

$$\omega_q < -\frac{1}{3},$$

which is the condition for quintessence. In other words, in the anisotropic model, ω_q does not have to cross the phantom divide.

Remark: The parameter α could be negative. For example, if $\alpha < -1$, we return to $\omega_q < -1$.

4 Wormhole structure

In this section we let $A = A_i, i = 1, 2$. Returning to the shape function $b(r) = D/r^{A-1}$, to meet the condition $b(r_0) = r_0$, we must have $D = r_0^A$. So the radius of the throat is $r_0 = D^{1/A}$ and

$$b(r) = r \left(\frac{r_0}{r} \right)^A.$$

Since $A > 0$, it now follows that $b'(r_0) < 1$, thereby satisfying the flare-out condition. From Ref. [1], we therefore obtain the “exoticity condition”

$$\frac{b(r_0) - r_0 b'(r_0)}{2[b(r_0)]^2} = \frac{A}{2r_0^2} > 0,$$

which shows that the weak energy condition has been violated. We already checked the asymptotic flatness, so that our solution describes a static traversable wormhole supported by quintom dark energy.

As discussed in Ref. [1], one can picture the spacial shape of a wormhole by rotating the profile curve $z = z(r)$ about the z -axis. This curve is defined by

$$\frac{dz}{dr} = \pm \frac{1}{\sqrt{r/b(r) - 1}} = \pm \frac{1}{\sqrt{r^A/D - 1}}. \quad (21)$$

For example, choosing $A = \frac{1}{2}$, we find that

$$z = 4\sqrt{D} \left[\frac{1}{3}(\sqrt{r} - D)^{3/2} + D\sqrt{(\sqrt{r} - D)} \right]. \quad (22)$$

The profile curve is shown in Figure 1 and the embedding diagram in Figure 2. The proper distance $l(r)$ from the throat to a point outside is given by

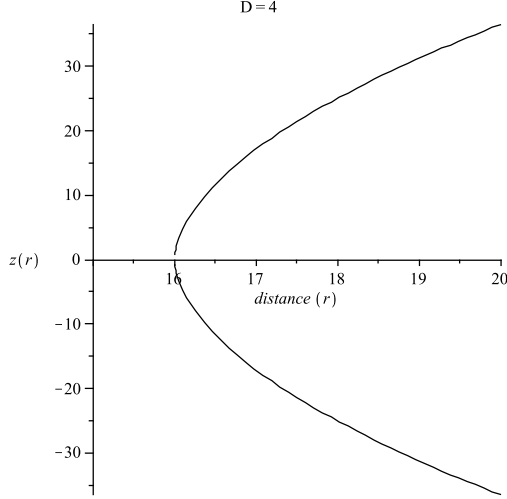


Figure 1: The profile curve of the wormhole.

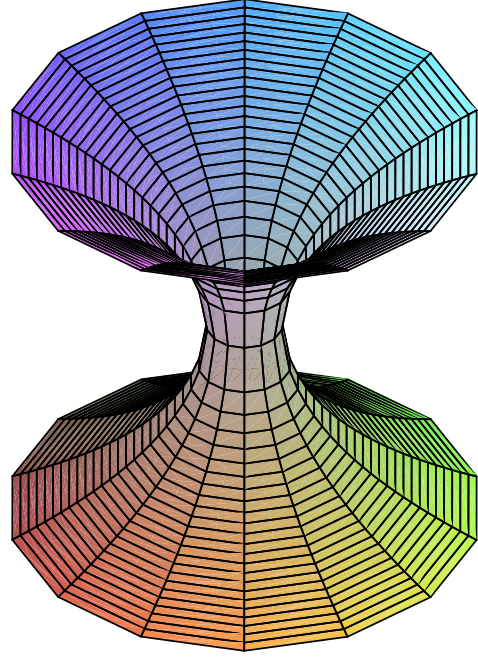


Figure 2: The embedding diagram generated by rotating the profile curve (fig 1) about the z -axis.

$$l(r) = \pm \int_{r_0^+}^r \frac{dr}{\sqrt{1 - b(r)/r}}. \quad (23)$$

For $A = \frac{1}{2}$,

$$l(r) = r^{1/4}(\sqrt{r}-D)^{3/2} + \frac{5D}{2}r^{1/4}(\sqrt{r}-D)^{1/2} + \frac{3}{2}D^2 \ln \left| \frac{r^{1/4} + (\sqrt{r}-D)^{1/2}}{\sqrt{D}} \right|. \quad (24)$$

(See Figure 3.)

It is customary to join the interior solution of a wormhole to an exterior Schwarzschild solution at some $r = a$. To do so, we demand that g_{tt} and g_{rr} be continuous at $r = a$:

$$g_{tt(int)}(a) = g_{tt(ext)}(a)$$

and

$$g_{rr(int)}(a) = g_{rr(ext)}(a);$$

$g_{\theta\theta}$ and $g_{\phi\phi}$ are already continuous [20]. So $e^{\nu_0} = 1 - \frac{2GM}{a}$ and $1 - \frac{b(a)}{a} = 1 - \frac{2GM}{a}$.

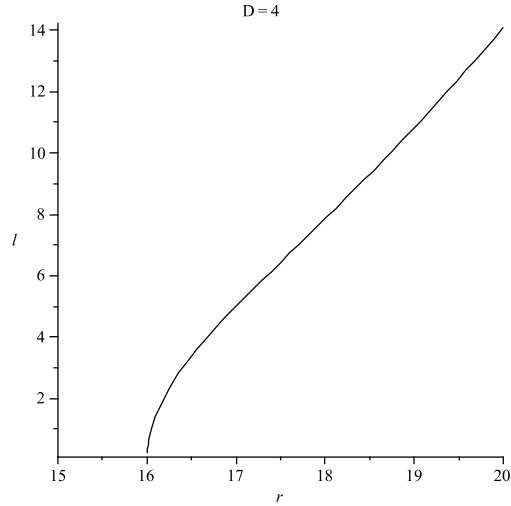


Figure 3: The graph of the radial proper distance $l(r)$.

This, in turn, implies that $D/a^{A-1} = 2GM$. and Hence, the matching occurs at

$$a = \left(\frac{D}{2GM} \right)^{1/(A-1)}. \quad (25)$$

The interior metric ($r_0 < r \leq a$) is given by

$$ds^2 = - \left[1 - \frac{D}{a^A} \right] dt^2 + \frac{dr^2}{1 - D/r^A} + r^2(d\theta^2 + \sin^2\theta d\phi^2) \quad (26)$$

and the exterior metric ($a < r < \infty$) by

$$ds^2 = - \left[1 - \frac{D}{a^{A-1}r} \right] dt^2 + \frac{dr^2}{1 - D/a^{A-1}r} + r^2(d\theta^2 + \sin^2\theta d\phi^2). \quad (27)$$

5 Model 2: A specific shape function

Returning to the isotropic case $p = p_r = p_t$, let us eliminate ρ and ρ_q in Eqs. (7) - (9) to obtain the following master equation:

$$\begin{aligned} & \frac{1}{4}(\nu')^2 + \frac{1}{2}\nu'' + \nu'g(r) \\ &= -\frac{e^\lambda}{2r} \frac{(\omega_{ph} + 1) + 3\omega_{ph}(\omega_q + 1)}{\omega_{ph} + 1} f(r), \end{aligned} \quad (28)$$

where

$$g(r) = -\frac{\lambda'}{4} + \frac{1}{2r} + \frac{3\omega_q + 1}{2r} - \frac{3\omega_{ph}(\omega_q + 1)}{2(\omega_{ph} + 1)r} \quad (29)$$

$$f(r) = (e^{-\lambda})' + \frac{A_1 e^{-\lambda}}{r} - \frac{A_1}{r}. \quad (30)$$

As in Eq. (13),

$$A_1 = \frac{(3\omega_q + 1)(\omega_{ph} + 1)}{(\omega_{ph} + 1) + 3\omega_{ph}(\omega_q + 1)}. \quad (31)$$

Now we choose the shape function $b(r)$ in such a way that the right-hand side of Eq. (28) is zero. For this specific choice, one gets the following solution:

$$e^{-\lambda} = \frac{1}{1 - b(r)/r} = 1 - \frac{D}{r^{A_1}}, \quad (32)$$

where $D > 0$ is an integration constant. Fortunately, this form is the same as in Model 1. So the physical characteristics, such as the profile curve, the embedding diagram, and the proper radial distance, remain the same. But the redshift function and stress-energy components are different.

By making the proper substitutions, one gets from Eq. (28)

$$\nu'' + \frac{\nu'}{r} \left[\frac{A_1 D}{2(r^{A_1} - D)} + L_1 \right] = -\frac{(\nu')^2}{2}, \quad (33)$$

where

$$L_1 = (3\omega_q + 2) - \frac{3\omega_{ph}(\omega_q + 1)}{(\omega_{ph} + 1)}. \quad (34)$$

Solving this equation, we get

$$\nu = \ln \left[E D A_1 + \sqrt{1 - \frac{D}{r^{A_1}}} \right]^2, \quad (35)$$

where E is an integration constant. We have used the condition $L_1 = A_1 + 1$. Starting with $L_1 - 1 = A_1$ and simplifying, one can readily deduce that $\omega_q = \omega_{ph}$; so once

again, $\omega_q < -1$, thereby having crossed the phantom divide. This is consistent with the isotropic case discussed in Subsection 3.1. (There is a similar consistency with the anisotropic case, as shown at the end of the present section.)

Finally, we get the following forms for ρ and ρ_q :

$$8\pi G\rho = -\frac{DA_1}{(1+\omega_{ph})r^{A_1+2}} \times \left[\frac{A_1 DE r^{A_1/2}}{\sqrt{(r^{A_1-D})} + A_1 DE r^{A_1/2}} \right] \quad (36)$$

and

$$8\pi G\rho_q = \frac{D(-A_1+1)}{r^{A_1+2}} + \frac{DA_1}{(1+\omega_{ph})r^{A_1+2}} \left[\frac{A_1 DE r^{A_1/2}}{\sqrt{(r^{A_1-D})} + A_1 DE r^{A_1/2}} \right]. \quad (37)$$

In the anisotropic case $p_t = \alpha\rho$, $\alpha > 0$, eliminating ρ and ρ_q in Eqs. (7)-(9) yields

$$\frac{1}{4}(\nu')^2 + \frac{1}{2}\nu'' + \nu'g(r) = -\frac{e^{-\lambda}}{2r} \frac{(\omega_{ph}+1) + 2\alpha + \omega_{ph}(3\omega_q+1)}{\omega_{ph}+1} f(r), \quad (38)$$

where

$$g(r) = -\frac{1}{4}\lambda' + \frac{1}{2r} + \frac{3\omega_q+1}{2r} - \frac{\omega_{ph}(3\omega_q+1) + 2\alpha}{2(\omega_{ph}+1)r} \quad (39)$$

and

$$f(r) = (e^{-\lambda})' + \frac{A_2 e^{-\lambda}}{r} - \frac{A_2}{r}; \quad (40)$$

here A_2 is defined in Eq. (19). In Eq. (33), A_1 is replaced by A_2 and L_1 by

$$L_2 = 1 + (3\omega_q + 1) - \frac{\omega_{ph}(3\omega_q + 1) + 2\alpha}{\omega_{ph} + 1}. \quad (41)$$

From the condition $L_2 - 1 = A_2$, we deduce that

$$\omega_q = \frac{\omega_{ph} + 2\alpha}{3}.$$

Since $\omega_{ph} < -1$ and $\alpha > 0$, we obtain, once again,

$$\omega_q < -\frac{1}{3}.$$

6 Discussion

The combination of quintessence and phantom energy in a joint model is referred to as quintom dark energy. The quintessence-like field is characterized by a free parameter ω_q with the restriction $\omega_q < -1/3$. For the corresponding free parameter ω_{ph} in the phantom-like field, the condition is $\omega_{ph} < -1$.

We have proposed in this paper that traversable wormholes may be supported by quintom dark energy. Two models were considered. The first model, a constant redshift function, leads to the determination of the shape function $b = b(r)$, which meets the flare-out conditions. The resulting space-time is asymptotically flat. This was followed by a brief discussion of the wormhole structure, including an embedding diagram, proper distance, and a junction to an external Schwarzschild spacetime. For the second, more general model, it is possible to use the same shape function but with a different redshift function and stress-energy components.

In each of these models, both isotropic and anisotropic pressures were considered. In the isotropic case, the phantom-energy condition $\omega_{ph} < -1$ implies that $\omega_q < -1$, and in the anisotropic case, $\omega_{ph} < -1$ implies that $\omega_q < -1/3$.

Acknowledgments

FR wishes to thank UGC, Government of India, for providing financial support. FR is also grateful for the research facilities provided by IMSc.

References

- [1] M.S. Morris and K.S. Thorne, Am. J. Phys. 56, 395 (1988).
- [2] A.G. Riess, *et al.*, Astron. J. 116, 1009 (1998).
- [3] S.J. Perlmutter, *et al.*, Astrophys. J. 517, 565 (1999).
- [4] O.B. Zaslavskii, Phys. Rev. D 72, 061303 (2005).
- [5] F.S.N. Lobo, Phys. Rev. D 71, 084011 (2005).
- [6] P.K.F. Kuhfittig, Class. Quantum Grav. 23, 5853 (2006); F. Rahaman, *et al.*, Phys. Lett. B 633, 161 (2006); F. Rahaman, *et al.*, Phys. Scripta 76, 56 (2007); F. Rahaman, *et al.*, Gen. Rel. Grav. 39, 145 (2007).
- [7] B. Feng, X. Wang, and X. Zhang, Phys. Lett. B 607, 35 (2005).
- [8] J.-Q. Xia, Y.-F. Cai, T.-T. Qiu, G.-B. Zhao, and X.-M. Zhang, arXiv: astro-ph/0703202.
- [9] G.-B. Zhao, J.-Q. Xia, M. Li, B. Feng, and X. Zhang, Phys. Rev. D 72, 123515 (2005).
- [10] R.R. Caldwell and M. Doran, Phys. Rev. D 72, 043527 (2005).
- [11] A. Vikman, Phys. Rev. D 71, 023515 (2005).
- [12] W. Hu, Phys. Rev. D 71, 047301 (2005).
- [13] M. Kunz and D. Sapone, Phys. Rev. D 74, 123503 (2006).
- [14] Y.-F. Cai, T. Qiu, R. Brandenberger, Y.-S. Piao, and X. Zhang, JCAP 0803, 013 (2008).
- [15] Z.-K. Guo, Y.-S. Piao, X. Zhang, and Y.-Z. Zhang, Phys. Lett. B 608, 177 (2005).
- [16] Y.-F. Cai, T. Qiu, Y.-S. Piao, M. Li, and X. Zhang, JHEP 0710, 071 (2007).
- [17] W. Zhao and Y. Zhang, Phys. Rev. D 73, 123509 (2006).
- [18] P. Moyassari and M.R. Setare, Phys. Lett. B 674, 237 (2009).
- [19] V.V. Kiselev, Class. Quant. Grav. 20, 1187 (2003).
- [20] J.P.S. Lemos, F.S.N. Lobo, and S.Q. de Oliveira, Phys. Rev. D 68, 064004 (2003).